

Active Tensegrity Structure

Etienne Fest¹; Kristina Shea²; and Ian F. C. Smith, M.ASCE³

Abstract: Most active structures involve direct control of single parameters when there is a closed form relationship between the response required and the control parameter. Building on a previous study of an adjustable structure, this paper describes geometric active control of a reusable tensegrity structure that has been enlarged to five modules with improved connections and is equipped with actuators. Closely coupled strut and cable elements behave nonlinearly (geometrically) even for small movement of the 10 telescopic struts. The control criterion for maintaining the upper surface slope has no closed form relationship with strut movement. The behavior of the structure is studied under 25 load cases. A newly developed stochastic search algorithm successfully identifies good control commands following computation times of up to 1 h. Sequential application of the commands through sets of partial commands helps to avoid exceeding limits during intermediate stages and adds robustness to the system. Reuse of a previously calculated command reduces the response time to less than 1 min. Feasible storage and reuse of such commands confirm the potential for improving performance during service.

DOI: 10.1061/(ASCE)0733-9445(2004)130:10(1454)

CE Database subject headings: Space structures; Tension; Control; Tests.

Introduction

Even though they were invented 40 years ago [Emmerich 1964; Fuller [U.S. Patent No. 3,063,521 (1962)]; Snelson [U.S. Patent No. 3,169,611,(1965)], tensegrity structures cannot be yet qualified as useable permanent structural systems. Currently, their construction is limited to creating sculptures and temporary structures for exhibitions. Giving tensegrity structures capabilities to maintain serviceability criteria may extend their usefulness. R. Buckminster Fuller, one of the inventors, described tensegrities poetically as “small islands of compression in a sea of tension.” Except for the visual metaphor that explains its principle of rigidity, contemporary engineers do not agree on a universal definition of tensegrities. A controversial aspect is whether compression members are connected. Motro (2002) proposed a broad definition of the tensegrity state: “A tensegrity state is a stable self-equilibrated state of a system containing a discontinuous set of compressed components inside a continuum of tensioned component.” Since

this definition includes structures in which compression members join, and since buckling of compression members is often critical, more efficient structures would fall into this category of structures (Robbin 1996; Wang 2002).

Tensegrities are lightweight space reticulated structures that can be easily dismantled and, therefore, provide innovative possibilities for reusable modular structures. Potential applications are temporary exhibition roofs (Pedretti 1998), radio telescopes, spatial deployable masts (Tibert 2002), air wings (Skelton et al. 2001b,) and space antennas. In contrast with tensile membrane structures, tensegrities self-stressing characteristic means that they do not need massive anchorage of compression rings. Nevertheless, tensegrities are recognized as being efficient structural systems (Motro 2003) and the number of full-scale prototypes being built is increasing. The largest laboratory structure is a double layer grid whose rectangular configuration covers an area of 82 m² with a self-weight of 11 kg/m² (Raducanu and Motro 2001; Motro and Raducanu 2001). Few prototypes have been tested experimentally. Saitoh et al. (2001), through loading a tensegrity arch, showed that an analytical model of the arch was able to correctly reflect its real behavior. Except for a few experimental studies most of the research on tensegrities has focused on theoretical aspects. For example, studies have been carried out on the identification of self-stress states and infinitesimal mechanisms (Pellegrino and Calladine 1986; Vassart et al. 2000), morphology, analytical and numerical prestress characterization (Sultan et al. 2002), dynamic behavior (Murakami 2001), tensegrity masts (Micheletti 2003) and deployable structures (Furuya 1992; Le Saux et al. 1999). The tensegrity configurations even arouse the interest of biologists who use them for modeling and explaining cell shape deformation (Ingber 1998).

Tensegrities are flexible structures and are sensitive to asymmetric loads and small environmental changes. Thus, they are often governed by serviceability criteria. Adaptation by changing their self-stress states provides opportunities, to meet such criteria. Equipped with sensors and actuators, active tensegrities provide the potential to control their shape and adapt to changing

¹Research Associate, Structural Engineering Institute, Applied Computing and Mechanics Laboratory, Structural Engineering Institute, School of Architecture, Civil and Structural Engineering (IMAC-IS-ENAC), Swiss Federal Institute of Technology (EPFL), 1015 Lausanne, Switzerland. E-mail: etienne.fest@epfl.ch

²Lecturer, Engineering Dept., Cambridge Univ., Cambridge, UK. E-mail: ks273@eng.cam.ac.uk

³Professor, Structural Engineering Institute, Applied Computing and Mechanics Laboratory, Structural Engineering Institute, School of Architecture, Civil and Structural Engineering (IMAC-IS-ENAC), Swiss Federal institute of Technology (EPFL), 1015 Lausanne, Switzerland. E-mail: ian.smith@epfl.ch

Note. Associate Editor: Satish Nagarajaiah. Discussion open until March 1, 2005. Separate discussions must be submitted for individual papers. To extend the closing date by one month, a written request must be filed with the ASCE Managing Editor. The manuscript for this paper was submitted for review and possible publication on June 2, 2003; approved on January 9, 2004. This paper is part of the *Journal of Structural Engineering*, Vol. 130, No. 10, October 1, 2004. ©ASCE, ISSN 0733-9445/2004/10-1454-1465/\$18.00.

tasks and environments (Shea et al. 2002). In this way, they have the potential, for example, to become part of an exhibition rather than merely provide shelter for one. Moreover, Skelton et al. (2001a b) demonstrated that in contrast to classical structures, tensegrities do not need excessive quantities of energy to ensure adequate control.

Until now, most structural control research in civil engineering has focused on active control of structures in order to enhance safety under extreme loading. While maintaining serviceability was mentioned in early work as a goal of structural control, there has been little investigation in this area (Shea et al. 2002).

Researchers have recently studied theoretically control of a tensegrity structure whose behavior is geometrically nonlinear and coupled. Djouadi (1998) focused on controlling the vibrations of four tensegrities modules that form a cantilever beam by changing their strut lengths. By changing strut lengths, Kanchanasatool and Williamson (2002) controlled the upper plane of a tensegrity module by linearizing the dynamics of the system. Their linearized model gave a good approximation of the nonlinear behavior of the structure. Sultan et al. (2002) controlled the shape of a one module tensegrity structure by changing cable lengths. They were able to control the height of the upper level under loading using symmetrical motion based on Lagrangian dynamics.

Experimental work that explored the active tensegrity potential was carried out by Fest et al. (2003) on a three module manually adjusted structure. The results were in contrast with the assumption of Kanchanasatool and Williamson (2002); nonlinear geometrical behavior occurs for cases of (i) small deflections, (ii) where loads are applied to several joints and (iii) when adjusting combinations of telescopic struts. Consequently, analytical simplification by superimposing strut length effects is not a reliable strategy by which to find an accurate control command. This previous work by the writers illustrated experimentally the potential for controlling tensegrity by manually adjusting strut lengths in order to maintain the slope of the upper level of a three module adjustable tensegrity structure. Since these systems exhibit geometrically nonlinear behavior and are strongly coupled, a stochastic search combined with dynamic relaxation was used to produce combinations of strut adjustments.

Tensegrities are good candidates for creating active structures. Aside from the structures in this project, no active tensegrity structure has been built that does not employ a linearized model for control. This paper builds on the work of Fest et al. (2003). The writers present in this paper a fully active tensegrity structure that is extended by two modules from the original three module configuration. The new prototype is an asymmetric configuration in which two modules do not touch supports and, therefore, this addition brings the prototype closer to a practical situation. The previous total surface area of 9 m^2 (three module structure) now has increased to 15 m^2 , including a wider unsupported span. This paper describes the active prototype, including the actuators and sensors which are embedded in a closed control loop, and advances in joint design. A quasistatic control strategy based on stochastic search is proposed and evaluated. Through testing of several load cases, the paper explores the benefits of embedding a control system in a tensegrity structure in order to satisfy the serviceability criterion.

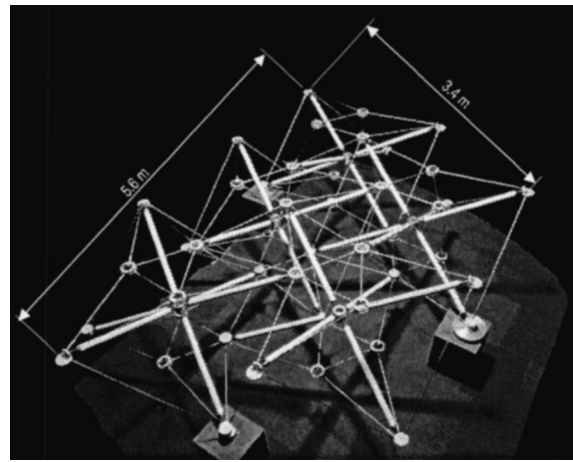


Fig. 1. Picture of five modules without actuators showing the three supports. Note that between modules, compression elements do not touch, that two modules are not supported and that the configuration is asymmetric.

Description of Tensegrity Structure

The prototype was designed and built at the Applied Computing and Mechanics Laboratory (IMAC) at the Swiss Federal Institute of Technology (EPFL) (Fig. 1) and was inspired by an original design by Passera and Pedretti (Pedretti 1998) for the Swiss National Exhibition. The structure consists of five modules arranged in an asymmetric configuration and contains connection module joints and center node designs that have been improved over those presented by Fest et al. (2003). Each module contains 6 struts and 24 cables. In contrast with classical tensegrity structures, a center joint is used to reduce the buckling length of compression members, thereby lowering the cross-sectional area required to avoid buckling of the struts. Telescopic struts, now active rather than adjustable members (Fest et al. 2003), are used to modify the geometry and self-stress in the system. Six mm diam stainless steel cables form a double-layered structure, where lateral cables connect top and bottom layers. Each layer is composed of two cable lengths, one forming three isosceles triangles and the other forming an equilateral triangle in the center; see Fig. 1.

When five modules are connected to create one tensegrity structure, the total number of joints is 51 and the number of tension and compression elements is 150. The height of the structure is 1.10 m and it weighs 30 kg/m^2 . Mechanical properties of struts and cables were not modified with extension from the three (Fest et al. 2003) to the five module configuration (Fest and Smith 2002). Six degrees of freedom are fixed at the three supports. Since the two modules in the middle are only connected to their neighboring modules and are not supported, this new configuration resembles a practical situation more closely than the three module structure (Fig. 2).

Both joint types have been improved over previous designs in order to increase stability and rigidity as well as to reduce frictional effects. Differences between measurements and the idealized structure are reduced by the following new design attributes:

- The six struts of each module meet at the center joint. This joint is composed of a lubricated steel ball that is in contact with the extremities of each strut [Fig. 3(b)]. The other end of the strut consists of a nut/threaded rod system to erect the

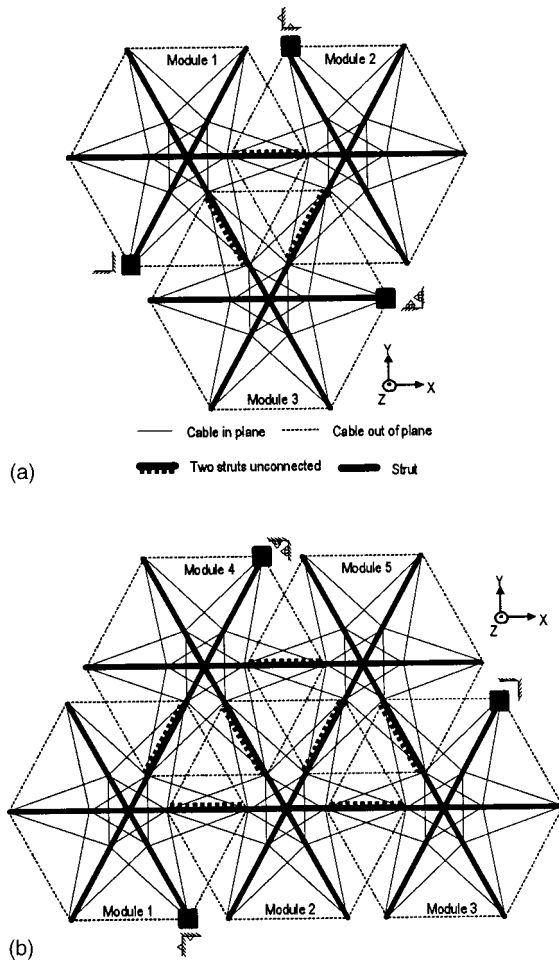


Fig. 2. Plan view: (a) three module structure, symmetric configuration (Fest et al. 2003); (b) five module structure, asymmetric configuration (note that modules 2 and 5 are not supported)

structure (Fest et al. 2003) using a simple wrench. Changing the strut lengths results in changing the amount of self-stress in the structure.

- In order to accommodate different connection situations between multiple cables and between cables and struts, a module-connection joint was created (Fig. 4). However, it could deform nonlinearly with changes in tension in the attached cables. In the new design, rings tie the joint together to limit this effect [Fig. 4(b)].

Control of Shape of Active Tensegrity Structure

Numerical Modeling

The tensegrity structure is equipped with sensors and actuators such that the shape and thus the behavior of the structure can be adapted. The way that shape control is carried out is schematically summarized in Fig. 5. The initial state of the structure is disturbed by a load. The structural response is then introduced as input to the search that combines a predictive model, *the analytic model*, with the search algorithm. Response displacements, δ_i , can be predicted from structural analysis as well as by measuring the structure under loading. The model is based on the geometry, topology and material properties of the structure analyzed using

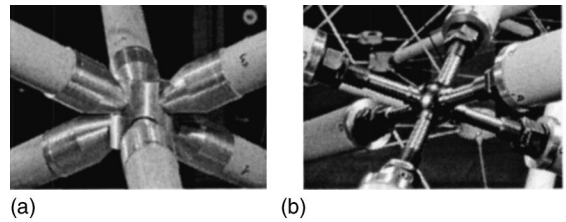


Fig. 3. Two stages of center joint development: (a) three module structure center joint (Fest et al. 2003) and (b) five module structure center joint

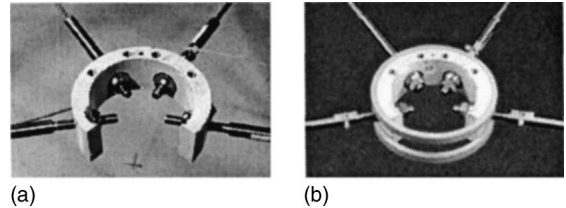


Fig. 4. Two stages of connection module joint: (a) three module structure open ring (Fest et al. 2003) and (b) five module structure closed ring

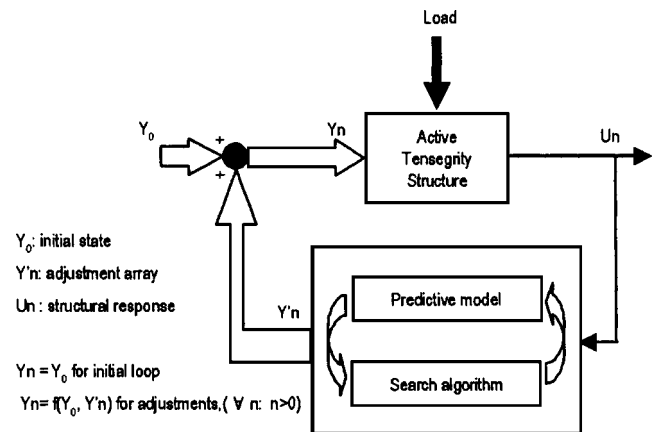


Fig. 5. Shape control loop (Fest et al. 2003)

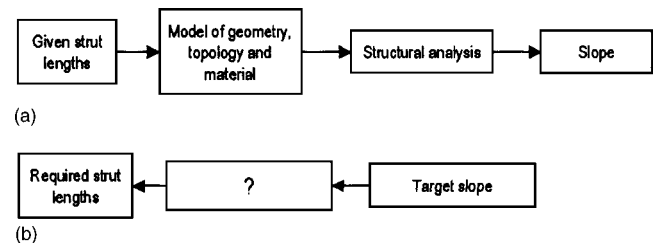


Fig. 6. Relationship between length of telescopic members and structure shape: (a) transformation from given structural geometry to slope and (b) transformation from target slope to required structural geometry

the dynamic relaxation method (Barnes 1977, 1999; Rossier 1993), a nonlinear analysis method, which has been shown to be reliable and accurate for this application (Fest et al. 2003).

The search is made by taking into consideration objectives and constraints, such as the slope and elastic limit of the cable. The search result consists of a set of strut elongations applied to the loaded structure. The new structural response is then measured to quantify the effectiveness of shape control.

Finding a good set of adjustment commands for the coupled, nonlinear system is a complex problem. There is no closed form solution for the system, that is, the relationship between inputs and outputs is not deterministic. For this reason, relating a target slope to a set of required struts lengths [Fig. 6(b)] is not as straightforward as determining the slope from given strut lengths [Fig. 6(a)]. The process that finds a control command consists of generating, analyzing and verifying a candidate command set.

Analyzing all theoretically possible commands is combinatorially explosive and leads to an exponentially increasing number of analyses with the number of active struts. A systematic search is required to determine which strut to change the length of and by how much. For this tensegrity structure, there are 10 active struts and the number of possible strut positions is determined by the range of movement, 50 mm, and the smallest allowed movement, 0.1 mm. This scenario results in over 9.75×10^{26} possible combinations of strut length. Placing constraints on the number of adjustable struts creates smaller solution spaces. As an estimate, each calculation takes 0.3 s. The time needed to test all possible solutions is estimated to be 9.29×10^{16} centuries.

Searching large solution spaces through stochastic search methods can identify beneficial adjustment commands (Fest et al. 2003). In that previous study a simulated annealing search was used. For the five module active structure described in this paper another stochastic search method, Probabilistic global search Lausanne (PGSL) (Raphael and Smith 2003), will be used, because it requires tuning only three search parameters to adapt to a new search task, whereas simulated annealing requires more (Domer et al. 2003b).

PGSL is a stochastic search algorithm based on the assumption that better sets of solutions are more likely to be found in the neighborhood of sets of good ones. Solutions are generated randomly in search space according to a probability density function (PDF), and they are evaluated using a user defined objective function. The user specifies the initial range of values of the parameters. The algorithm dynamically updates the PDF so that a more intensive search is carried out in regions containing good solutions.

Control Scenarios, Actuator Placement and Control Setup

In extending the three module structure to five modules, the initial control objective of maintaining a zero slope (Fest et al. 2003) has been modified. While the symmetric configuration of the three modules permits starting from a state where all response joints are at the same height, the asymmetric configuration and deformation from dead load and actuator weight now yield unequal initial heights of the response joints.

The goal of shape adjustment in this study is to maintain the initial slope of the structure on the upper level. Joints 37, 43, and 48 are chosen to represent the upper-level slope and form a triangle as indicated in Fig. 7. The scenario also corresponds to setting the structure at a target slope and maintaining that slope. The response joints are instrumented with three linear variable

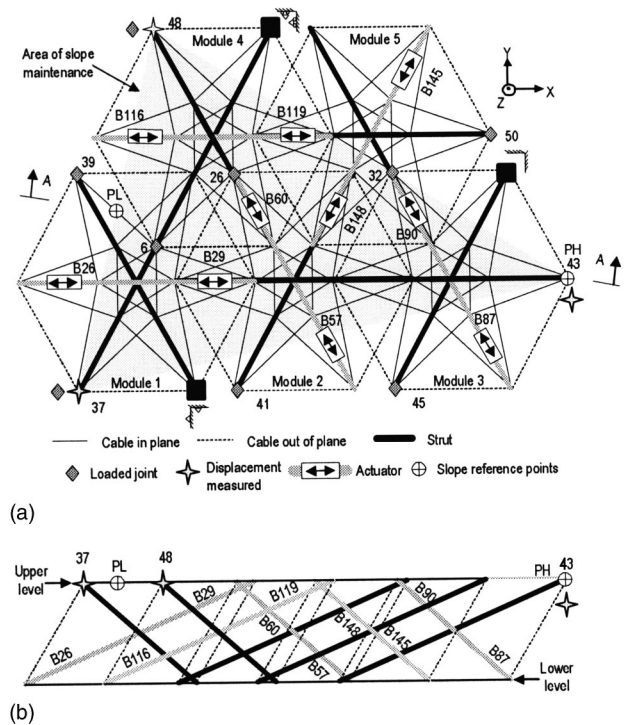


Fig. 7. Schematic of the structure: (a) plane view of sensor, load and control area location and (b) elevation view of sensor, load, level, and slope reference joint location

differential transformers (LVDTs) to measure vertical displacement, δ_i . The nominal accuracy of LVDTs is $\pm 10 \mu\text{m}$ and sensors are fixed to a rigid framework that encapsulates the entire structure (Fig. 8). The shape control task consists of changing the lengths of a number of telescopic struts so that the slope is maintained from the region of the high point (HP) (see Fig. 7), to the region of the low point (LP). The initial slope under dead load of the system, $\text{slope}_{\text{initial}}$ should be maintained (Fig. 9). In other words, deviation from the initial slope, Δslope [Eq. (1)], is calculated through concatenation of the relative vertical displacement of the three joints divided by the distance between HP and LP, $L_{\text{HP-LP}} = 4,600 \text{ mm}$, [Eq. (2)]. The $\text{slope}_{\text{modified}}$ is the slope modified by loading:

$$\Delta\text{slope} = \text{slope}_{\text{initial}} - \text{slope}_{\text{modified}} \quad (1)$$

$$\text{slope} = \frac{(\delta_{43} - \delta_{48} + \delta_{37}/2)}{L_{\text{LP-HP}}} \quad (2)$$

Maintaining the initial slope does not require that the upper layer of the structure return to its initial position after loading. Multiple solutions can also be found either above or below this position (Fig. 9).

For the five module tensegrity, 30 telescopic struts have the potential to be adjusted. The number of active struts has been chosen as 10, that is, two jacks located symmetrically along the same axis in each module (Fig. 7). Note that the system is under-actuated, since 10 active struts need to deal with a system with a larger number of degrees of freedom. The following aspects were considered in choosing the number of active struts and their location:

- Increasing the number of active struts from two to five per module does not necessarily lead to improved performance for this structure (Fest et al. 2003);



Fig. 8. Overall view of entire active control system

- It is desirable for a modular structure that the same struts in each module be made active so that individual modules can be constructed uniformly and then assembled on site;
- The choice of active struts is constrained by symmetry so that a similar arrangement should be applicable when enlarging the structure to more than five modules;
- Strut movement should lead to the maximal number of lengthening directions of the structure and maximal coupling of active struts;
- Strut movement is possible on both the lower and the upper level;
- The three struts that are connected to supports cannot be moved; and
- The three struts that are fixed to response joints are not active.

It is worth mentioning that placing actuators in a line along a common axis also reduces displacement of the center node (compared with only one actuator), thereby diminishing an important cause of geometrical nonlinear behavior, and stabilizing the structure.

An actuator consists of an electromechanical jack which produces linear energy by rotary energy (Fig. 10). Rotary energy is created by an electric asynchronous motor via a bevel gear system (worm and wheel) and a screw nut system. Each actuator is equipped with a LVDT to measure displacement of the piston, which is continuation of the screw. The LVDT is used as a feedback control sensor. For unpredictable situations, the piston stroke displacement is bounded by a displacement limiter which, when touched, shuts off the motor.

To ensure a safe and rapid control system, all the devices are multiplexed on a serial bus. The control area network (CAN) (Bosch 1993) bus, under CANopen protocol enables one to communicate in real time between devices. Information is provided via a PC interface card run by a program written in LabView (Fig. 11). The program permits automated application of a control command. Automatic override is built into the program which will

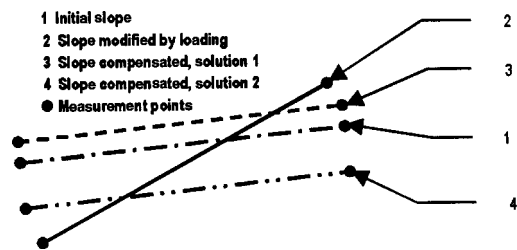


Fig. 9. Two-dimensional schematic of slope maintenance: view A-A (Fig. 7).

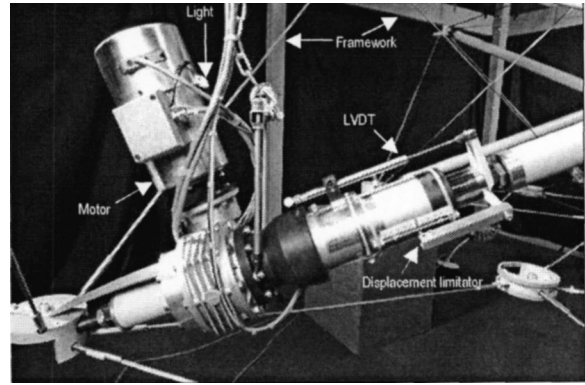


Fig. 10. Elevation of an actuator set in a strut; note the LVDT and the displacement limitation device

cause the system to stand by if maximum stroke displacement is detected by a LVDT. More detailed information of the active system configuration was given by Fest (2002).

Additional weight (400 N) and rigidity of the jack need to be added to the analytic model. While the bending deformation of the active strut associated with the dead load of the jack is very small, we considered only the unilateral rigidity of the struts. Rigidity is determined by calculating an equivalent Young's modulus of the strut assuming an undeformable jack. The jack weight is distributed to the two element nodes in proportion to the position of the center of gravity of the ends of the active strut.

The nominal initial length of the struts is 1,296 mm. For these tests, a 2.5 mm prestress position, which corresponds to strut lengths of 1,298.5 mm, is taken to be the zero position. Each active strut can then either be lengthened or shortened in discrete increments that are determined from the LVDT level of accuracy. In order to avoid maximum stress and critical buckling force, changes in strut length are restricted to ± 25 mm. The stress allowed in cables, 163 MPa, against yielding incorporates a safety factor of 2. The maximum compressive force in struts, 20 kN, is based on experimental tests on 1-m struts. With the new control objective, a constraint has been added. It ensures minimum strut compressive force, thus avoiding tension in the struts. This value has been fixed to 2 kN. Moreover, considering LVDT accuracy in measuring displacement, the minimizing process of the stochastic

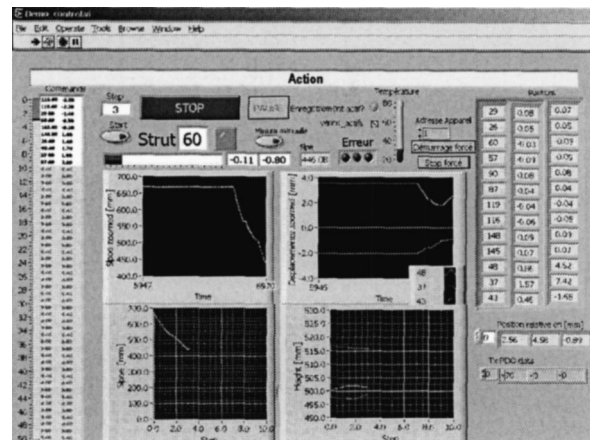


Fig. 11. Control front panel

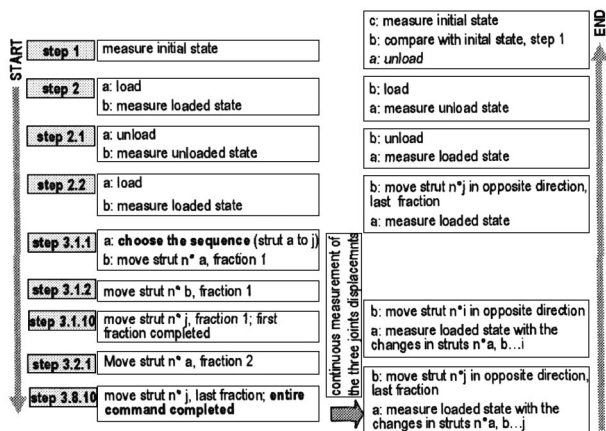


Fig. 12. Testing procedure

search. [Eq. (2)] is stopped upon achieving a threshold. This value is fixed at 4.35×10^{-4} . Note that self-weight causes an initial slope of 24.57×10^{-4} .

Activation and Movement Strategy

Quasistatic control is based on a two step strategy.

- Split a control movement into a sequence of smaller movements. Given a command consisting of a set of strut adjustments, the experimental testing procedure is described in Fig. 12. Considering possible 25-mm strut elongation, applying a control command at once might cause instability due to the bucking of passive struts or cable yield. The control command is divided into parts so that no movement exceeds a maximal increment of 3.2 mm. This value is calculated using the testing safety margin.
- Apply commands sequentially until the complete command is reached. Struts are moved one by one and the sequence is fixed in order to minimize the energy in the structure; thus, shortening movements are carried out prior to lengthening ones.

Since, during each step, only one active strut is allowed to move, the maximum number of steps to complete the command is 80. This number is calculated by multiplying the number of active struts (two per module times five modules) by 25 and dividing by 3.2. Due to geometrical nonlinearity, intermediate stages may nevertheless overstress some elements. The effect of each stage along the path is simulated in order to avoid such problems. When a simulated intermediate stage overstresses an element, the sequence is changed.

The procedure for testing a single set of hypothetical adjustments for Struts A–J is illustrated in Fig. 12. This testing procedure is an improvement over the one used with the adjustable tensegrity structure (Fest et al. 2003) due to continuous measurement that enables one to detect intermediate states that could meet the control objective. Also, since the path is governed by the minimum energy introduced into the structure, applying a command is now safer. It is necessary to split commands into fractions since overall movement is larger in these tests.

Load Cases

This kind of tensegrity structure is more sensitive to asymmetric edge load cases than uniform or top/center load cases (Fest et al. 2003). Accordingly, loads are applied to the upper level structure

edges. Twenty-five load cases are considered, including single point loads and two point loads (Table 1). The loads are applied in the negative Z direction. Since geometrical nonlinearity and coupling effects are significant even for small structure deformation and small changes in strut length and since the goals of these tests do not include measuring the structural capacity, the maximal loads magnitude applied to a single joint is limited to 1,092 N. A range of load magnitudes is applied to each joint selected. Load cases were selected in order to create appropriate and comparable slopes for the different load cases ($8.69, 13.04, \text{ and } 16.30 \times 10^{-4}$) and enable demonstration of the sensitivity of the reference triangle to the load positions. As shown in Table 1, the slope is most sensitive to a one point load where load is applied to Joint 48, resulting in a slope response of 16.72×10^{-4} . For each load case, the test is carried out three times. The minimum load magnitude is determined from the repeatability of the tests. Considering maximal standard deviation of 2.17×10^{-5} of the measured slope among all load cases, the minimal slope created by a load case is 6.52×10^{-4} . The factor of 30 corresponds to twice the standard deviation of the three sets of measurements times a factor of 15; such factors limit the noise for better test repeatability.

Results

We now describe an investigation of the slope control of the structure through comparison of experimental testing and numerical analysis. Experimental tests were carried out three times for each load case.

Correlating Predictions with Measurements for the Initial Slope

Control commands applied to the structure are based on the predicted response calculated by dynamic relaxation. Fig. 13 indicates the initial correlation between Δ slope predicted by the analytic model and Δ slope measured on the structure for each load case, calculated using Eq. (3), before applying a control command. Values of correlation close to 100% indicate that the deviation is insignificant in Fig. 13, correlation histogram values superior to 95% are not labeled.

$$\text{Initial correlation (\%)} = \left(1 - \left| \frac{\Delta \text{slope}_{\text{measured}} - \Delta \text{slope}_{\text{predicted}}}{\Delta \text{slope}_{\text{predicted}}} \right| \right) \times 100 \quad (3)$$

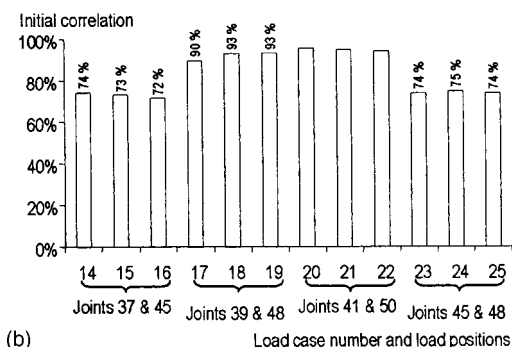
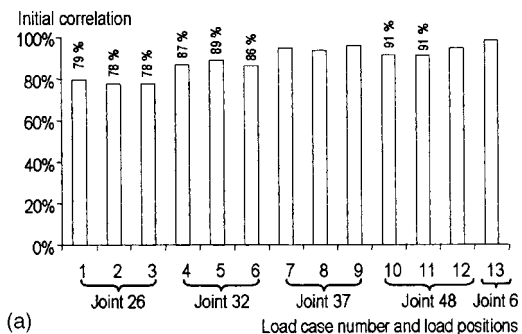
$$\text{Deviation (\%)} = 100 - \text{initial correlation} \quad (4)$$

For single point load cases, Fig. 13(a) shows that the initial correlation is at least 78%. Moreover, the correlation is almost uniform for different magnitude loads applied at the same location. The average deviation is insignificant with regard to the loads applied to Joint 37 (5%) and is low with regard to the loads applied to Joint 48 (8% average) since they are edge loads and produce the largest displacement. It increases slightly for load applied at Joint 32 (13% average). Applying loads at joints connected to an actuator causes the largest deviations between prediction and measurements (Load Cases 1–6, Joints 32 and 26).

For double point load cases, Fig. 13(b) shows that the initial correlation is at least 72%. Moreover, the correlation is almost uniform for different magnitude loads applied at the same location. Although loaded joints do not belong to measured modules, the deviation is insignificant with regard to the loads applied simultaneously at Joints 41 and 50 (<5%) (Load Cases 20–22).

Table 1. Load Cases

| Load case type | Loaded joint number | Load (N) | Module number | Simulated slope (10^{-4}) | Actuator connected |
|--------------------------|---------------------|----------|---------------|-------------------------------|--------------------|
| Single point load | | | | | |
| 1-central | 26 | 625 | 1 and 2 | -8.98 | Yes |
| 2-central | 26 | 900 | 1 and 2 | -12.61 | Yes |
| 3-central | 26 | 1209 | 1 and 2 | -16.52 | Yes |
| 4-central | 32 | 625 | 3 and 5 | -9.50 | Yes |
| 5-central | 32 | 859 | 3 and 5 | -12.98 | Yes |
| 6-central | 32 | 1092 | 3 and 5 | -16.37 | Yes |
| 7-asymmetric | 37 | 391 | 1 | -9.06 | no |
| 8-asymmetric | 37 | 550 | 1 | -12.80 | No |
| 9-asymmetric | 37 | 700 | 1 | -16.35 | No |
| 10-asymmetric | 48 | 391 | 4 | -9.3 | No |
| 11-asymmetric | 48 | 550 | 4 | -13.11 | No |
| 12-asymmetric | 48 | 700 | 4 | -16.72 | No |
| 13-central | 6 | 1092 | 1 and 4 | -9.00 | no |
| Two point load | | | | | |
| 14-longitudinal | 37 and 45 | 391 | 1 and 3 | -8.35 | No |
| 15-longitudinal | 37 and 45 | 624 | 1 and 3 | -13.20 | No |
| 16-longitudinal | 37 and 45 | 742 | 1 and 3 | -15.63 | No |
| 17-asymmetric | 39 and 48 | 157 | 1 and 4 | 9.24 | No |
| 18-asymmetric | 39 and 48 | 215 | 1 and 4 | 12.67 | No |
| 19-asymmetric | 39 and 48 | 274 | 1 and 4 | 16.15 | No |
| 20-coupling | 41 and 50 | 391 | 2 and 5 | 8.63 | No |
| 21-coupling | 41 and 50 | 624 | 2 and 5 | 13.37 | No |
| 22-coupling | 41 and 50 | 742 | 2 and 5 | 15.63 | No |
| 23-transversal | 45 and 48 | 391 | 3 and 4 | -8.61 | No |
| 24-transversal | 45 and 48 | 624 | 3 and 4 | -13.61 | no |
| 25-transversal | 45 and 48 | 742 | 3 and 4 | -16.11 | No |

**Fig. 13.** Correlation between the predicted and measured slope of (a) single load cases and (b) double load cases

The deviation between prediction and measurement is low with regard to the loads applied simultaneously at Joints 39 and 48 (average 8%) (Load Cases 17–19). It increases for longitudinal and transversal load cases (Joints 37 and 45 and Joints 45 and 48) (average 27–26%, respectively). Comparing initial correlation for loads applied at Joints 37, 48, 37, and 45 and 45 and 48, loading Joint 45 leads to the largest deviations. Considering all load cases, it is noteworthy that the LVDT accuracy influences slope measurement more for low load magnitudes. Moreover, correlation variation may be caused by joint friction.

Slope Control

The goal of shape control can be defined as maintaining the slope of the upper level of the structure through changing combinations of strut lengths. The response of the controlled structure, as calculated by the equation below, is used to evaluate the effectiveness of sets of strut adjustment. Data are provided by measurements of the structure. The initial slope $\text{slope}_{\text{initial}}$ is the slope under dead of the system. The variable, $\text{slope}_{\text{modified}}$, is the slope modified by loading. The variable, $\text{slope}_{\text{adjusted}}$, is the slope modified by loading and corrected by a command determined by the search.

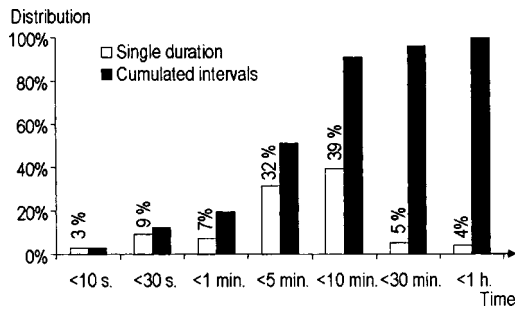


Fig. 14. Distribution of the search time in duration intervals

Slope compensation (%)

$$= \left(1 - \left| \frac{\text{slope}_{\text{initial}} - \text{slope}_{\text{adjusted}}}{\text{slope}_{\text{initial}} - \text{slope}_{\text{modified}}} \right|_{\text{measured}} \right) \times 100 \quad (5)$$

It is noteworthy that all control commands did not require the same search time, that is, the execution time of PGSL, even when the search space was the same size (Fig. 14). Fig. 14 illustrates the search time distributed in duration intervals. The total number of PGSL search runs is 225, i.e., each of the 25 load cases was performed nine times. The white column represents the ratio (percentage) of the number of search processes completed within a time range and the total number of search processes completed in less time than the upper limit of the range. The dark column corresponds to the ratio of the accumulated number of search processes starting at time zero for a certain duration and the total number of search processes. For the 25 load cases, the search process was completed in less than 1 h (PC 2.2 GHz/512 MB). Fig. 14 indicates that most search processes (71%) were completed within 1–10 min, but nine search processes (4%) needed more than 30 min and can take almost 1 h. It is important to note that search time is linked to the complexity of the control objective as well as to the hardware. For comparison, Shea et al. (2002) have found that determining a set of adjustments to control the

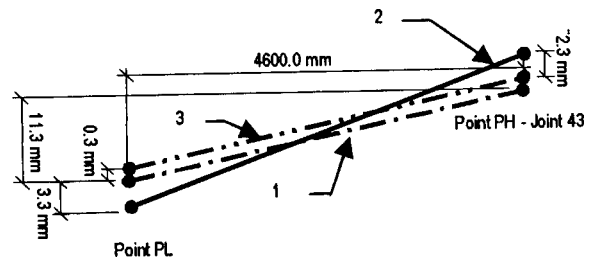


Fig. 15. Displacement and slope compensation for Load Case 8: view A-A, longitudinal to the control line

slope of a three module structure took approximately 160 min (Silicon Graphics octane 175 MHz/128 MB).

To give a more detailed example, a command generated by the search for Load Case 8 is listed in Table 2. The command (last row) is divided into three fractions with a maximal shortening change of -2.45 mm for lower case Strut 29 and extending change of 1.5 mm for Strut 148. Applying the command to the structure in 30 steps, starts with shortening Strut 29 by 2.45 mm and finishes by extending Strut 148 by 1.57 mm to achieve the final length. The initial and final deformation and slope are shown in Table 3. A graphic illustration of this is shown in Fig. 15.

In Fig. 16, values of slope compensation close to 100% indicate that the slope of the structure has returned to the desired slope. Slope compensation histogram values superior to 95% are not labeled and identify good control commands. Shape control in tested for 25 load cases. Slope compensation effectiveness is shown in Fig. 16(a) for single load cases. Applying a control command results in changes to the upper plane, enabling it to compensate at least 78% of the slope. For 9 load cases out of 13, the control commands determined are good (compensation $>95\%$ for Load Cases 1–6 and 10–12).

With regard to double point load cases, slope compensation effectiveness is shown in Fig. 16(b). For 10 load cases out of 12, the control command permits the structure to compensate for

Table 2. Example of Sequence of a Command Divided into Three Fractions, Load Case 8

| | | | | | | | | | | |
|-------------------------|-------|-------|-------|-------|------|-------|-----|-------|------|------|
| Strut number | 29 | 57 | 119 | 145 | 90 | 26 | 60 | 116 | 87 | 148 |
| Step | 1 | 2 | 3 | 4 | 5 | 6 | 7 | 8 | 9 | 10 |
| Command fraction 1 (mm) | -2.45 | -2.21 | -2.12 | -1.48 | -0.9 | -0.87 | 0.8 | 1.116 | 1.45 | 1.57 |
| Step | 11 | 12 | 13 | 14 | 15 | 16 | 17 | 18 | 19 | 20 |
| Command fraction 2 (mm) | -4.9 | -4.42 | -4.25 | -2.96 | -1.8 | -1.75 | 1.6 | 2.32 | 2.9 | 3.14 |
| Step | 21 | 22 | 23 | 24 | 25 | 26 | 27 | 28 | 29 | 30 |
| Entire command (mm) | -7.35 | -6.63 | -6.54 | -4.44 | -2.7 | 2.61 | 2.4 | 3.49 | 4.35 | 4.71 |

Table 3. Structure Deformation and Slope for Command Given in Table 2

| | Modified state | | | Slope (10^{-4}) | Compensated state | | | Slope (10^{-4}) | Slope compensation (%) |
|--------------------------------|-------------------------------|-------|-------|------------------------|-------------------------------|-------|-------|------------------------|---------------------------|
| | Joint height δ (mm) | | | | Joint height δ (mm) | | | | |
| Initial slope (10^{-4}) | 37 | 48 | 43 HP | 37.39 | 37 | 48 | 43 HP | 24.56 | 99 |
| 24.57 | 498.8 | 500.6 | 516.9 | 37.39 | 506.5 | 500.1 | 514.6 | 24.56 | 99 |

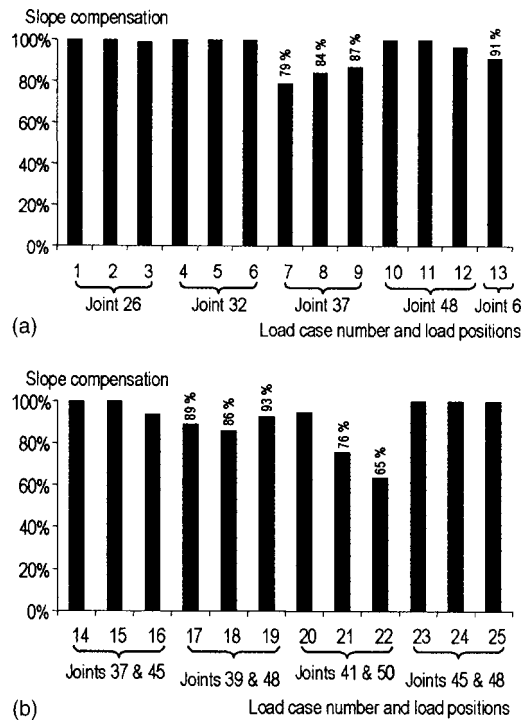


Fig. 16. Slope compensation for (a) single load cases and (b) double load case

more than 86% of the slope that was modified by loading. For 7 load cases of total of 12, the control commands applied are good (compensation >95% for Load Cases 14–16, 20, and 22–25).

Compensation effectiveness decreases for coupled load cases when the applied load magnitude is high, e.g., Load Cases 20–22. Slope compensation starts at 95% and goes down to 76% and finally reaches a minimum of 65%. In these load cases, the joints measured do not belong to the loaded modules. With regard to Load Case 22 (65% compensation), the sequence of applying the command may as well alter control. Nonlinear geometrical systems are sensitive to the sequence of loads applied.

With regard to all load cases, the quasistatic control strategy, consisting of dividing the command into sequences of parts, led to no difficulties in satisfying strength and buckling constraints, and it proved successful for meeting the control objectives. The analytic model, which incorporates the active elements, is well suited for predicting the structure deformation. For all load cases, changing the strut lengths resulted in moving the upper level slope toward the initial slope. It shows that the combination of PGSL with dynamic relaxation has the potential for identifying goods sets of adjustments even in situations of nonlinear behavior and exponentially complex search spaces positioning actuators along the same line are well suited for this application. For all load

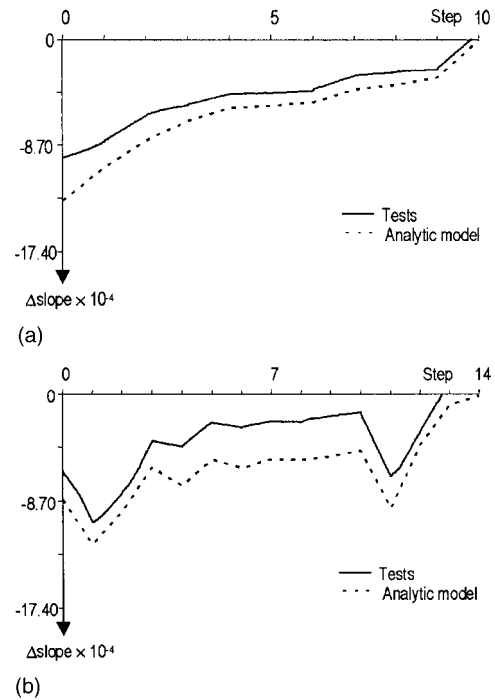


Fig. 17. Prediction and measurement of Δ slope [Eq. (1)] with iteration step: (a) single point load, Load Case 15 and (b) double point load, Load Case 23

cases, the results demonstrate that the actuator positions are well suited for the structure and control objective under study.

Robustness

In Fig. 17, lines are used to show the change in slope calculated by the analytic model and continuous lines represent the Δ slope measured. Fig. 16 has shown that good control commands exist and can be identified in order to ensure that serviceability criterion is met. It is interesting to explore how the initial correlation between prediction and measurement can affect the quality of slope compensation.

Comparison of Figs. 15(a) and 16(a) and of Figs. 15(b) and 16(b) shows that initial deviation between prediction and measurement does not necessarily lead to low slope compensation after applying a control command. With regard to Load Cases 1–3, although the average initial correlation is only around 78%, applying a control command modifies the slope and permits the structure to regain more than 95% of the initial slope. Fig. 17(a) shows that applying a command by steps makes the slope converge to the initial slope, even with an initial correlation of 78%. The vertical axes in Fig. 17 are the numbers in Eq. (5). Here, considering the changes in strut length predicted were all less

Table 4. Comparison of Command Predicted and that Applied (and Measured), Load Case 15

| Strut number | 26 | 119 | 29 | 116 | 60 | 148 | 87 | 145 | 57 | 90 |
|------------------------|-------|-------|-------|-------|------|------|------|------|------|------|
| Step | 1 | 2 | 3 | 4 | 5 | 6 | 7 | 8 | 9 | 10 |
| Command predicted (mm) | -2.7 | -2 | -1.5 | 0.9 | 0.3 | 0.6 | 0.8 | 0.9 | 1 | 2.4 |
| Command applied (mm) | -2.67 | -1.96 | -1.46 | -0.86 | 0.26 | 0.56 | 0.77 | 0.87 | 0.93 | 1.92 |

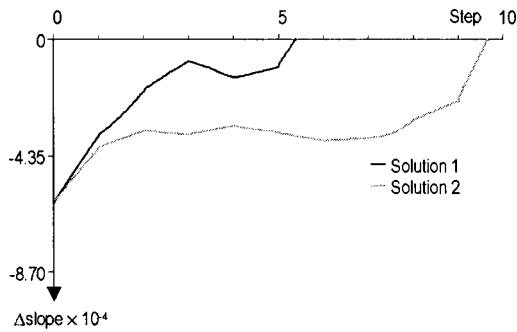


Fig. 18. Comparison of slope compensation evolution between two equivalent quality solutions, Load Case 14

than 3.2 mm, the command did not need to be factorized. In this load case, the entire command did not need to be applied since total slope compensation is achieved between Steps 9 and 10. The 10th fraction is only partially applied. Measuring the slope and strut length continuously during strut adjustments makes it possible to identify when the slope is completely compensated. Table 4 compares the command predicted and the command applied and measured on the structure. It shows that lengthening Strut 90 by 1.92 mm (80% of the predicted length) instead of 2.4 mm is enough to compensate for the slope.

With regard to Load Cases 23–25, although the average initial correlation was only around 73%, applying a control command led to more than 95% recovery of the initial slope. For example, in Load Case 23, an initial correlation of 78% was established between measurement and prediction. Fig. 17(b) shows that the command that is applied to the structure step by step enables complete compensation of the initial slope. In this load case, the entire command did not need to be applied, because full slope compensation is achieved between Steps 12 and 13. The 13th fraction is partially applied. With regard to the shape of the curves, some struts have a more prominent effect on slope variation than others.

Both Load Cases 15 and 23 show initial deviations between prediction and measurement that fortunately do not result in system divergence. Such robust behavior was observed repeatedly. The uncertainty does not accumulate throughout the adjustment; incremental adjustments bring the structure closer to its initial slope. For load cases where the initial correlation was below 85% (Load Cases 1–3, 10, 11, 14–19, and 22–25), the slope prediction was higher than the slope measured, i.e., the model predicts a more flexible structure than is really the case reality. For these load cases, the control command fully compensated the slope. When the control command is calculated for a structure more flexible than the real structure, it is likely that applying this command to the real structure has a positive effect on slope compen-

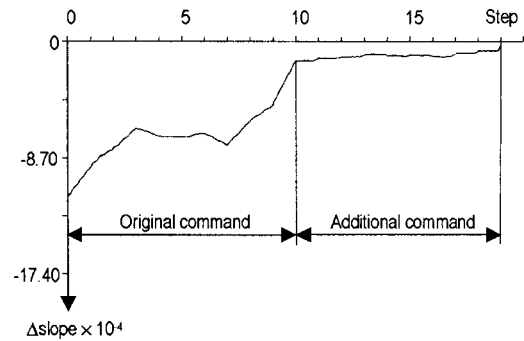


Fig. 19. Iterative slope compensation, Load Case 8

sation. Nevertheless, in cases of large initial deviations between predictions and measurements, this could be dangerous, since real forces in members would be underestimated.

Comparison of Two Solutions

As suggested in Fig. 9, multiple solutions exist and are found using a stochastic search (Fig. 18). To investigate the equivalence of predicted similar quality solutions, two solutions were tested on the structure for Load Case 14. As shown in Table 5, the commands are quite different. In comparing both commands, many of the struts that are adjusted are moved in opposite directions, thus illustrating that very different solutions are possible. For instance, Strut 116 should be shortened by 2.80 mm in Command 1, while Strut 116 should be lengthened by 0.5 mm in Command 2. Moreover, Command 1 only needs 6 active members while Command 2 needs 10 active members.

Considering slope compensation, both commands are effective and are applied only partially. Criteria that help to choose between the two commands can be formulated. For instance, solution 1 could be selected since it requires less energy or due to its proximity to the initial position of the struts. In summary, it is likely that for such a nonlinear system, a multicriteria search would be needed for control objectives that are associated with serviceability. This research is underway.

In situations where achieving the performance goal with just one command is not completely successful, opportunities exist for making further iterations beginning with the new deformed shape. Iterative control leads to an active structure that can be modified step, provided that convergence is probable. Three possible strategies for iterative control are discussed.

1. Strategy 1: Analyze the response of the structure to a control command in order to highlight which strut for this load case had the most influence on slope variation. A new command is built that allows only micromovement (± 1 mm) of struts starting with the most influential struts and stopping when

Table 5. Two Different Equivalent Quality Commands, Load Case 14

| | | | | | | | | | | |
|----------------|-------|-------|-------|------|------|------|-----|-----|-----|-----|
| Strut number | 116 | 26 | 119 | 26 | 145 | 87 | | | | |
| Step | 1 | 2 | 3 | 4 | 5 | 6 | | | | |
| Command 1 (mm) | -2.80 | -2.47 | -1.15 | 1.35 | 1.58 | 1.86 | | | | |
| Strut number | 26 | 29 | 145 | 60 | 119 | 57 | 87 | 116 | 80 | 148 |
| Step | 1 | 2 | 3 | 4 | 5 | 6 | 7 | 8 | 9 | 10 |
| Command 2 (mm) | -3 | -2.9 | -2.9 | -2.6 | -2.1 | -1.6 | 0.5 | 0.5 | 1.1 | 1.5 |

the initial slope is regained. This technique is intended for small slope compensations association with small strut movement. The effect of the additional commands is checked in order not to reach the material and geometrical limits of the structure.

2. Strategy 2: Use the original command and create a new one by scaling a command fraction in smaller steps. Starting at the final position resulting from the original command, parts of the command fraction are applied successively since the measurements show that the command enabled the structure to improve the slope. For instance, in Load Case 8, a single command enabled the structure to regain only 86% of its initial slope. The movements of each strut are calculated by multiplying the original command by 0.15. Applying an additional command based on the original calculated by the search algorithm enables the structure to reach maximal slope compensation (Fig. 19). Once again, the effect of the additional strut adjustments are checked in order to avoid reaching the material and geometrical capacities of the structure.
3. Strategy 3: Identify a new search command with the stochastic tool starting with the deformed shape. This strategy needs model calibration based on measurement within the search (Shea et al. 2002). Domer et al. (2003a,b) showed the potential of improving the prediction accuracy of the three module tensegrity structure model by comparing simulations to measured data. An artificial neural network trained with these data increased the model accuracy. A technique that couples stochastic search with model calibration is currently under development in order to integrate parameters that are difficult to mode, such as joint friction.

Strategies 1 and 2 proved successful for small strut length changes. However, it could be dangerous to use them in cases where there is large slope deviation after applying the original command, due to possibilities of overstressing the structure or decreasing the slope compensation. Strategy 3 would be safer for cases where 35% of the slope or more needs to be compensated after applying the original command. But Strategy 3 is slower since it requires a new search. Thus, a hybrid approach would take advantage of the three strategies and would be useful for a wide range of situations.

Considering all load cases, it is likely that information about good control commands associated with prediction, iterative control and continuous measurement would be helpful in finding a control command in a similar situation loading. Good control commands and their associated sequences are stored in order to be retrieved and reused in cases where the same load case reappears. Advantages of reusing good control commands are the following:

- No stochastic search;
- No need to verify intermediate states associated with applying strut adjustments one by one through fractioning the command; and
- Less risk of iterative control when the original command is not effective enough.

For all load cases, all good control commands and their associated sequences were stored and classified in independent files with names to describe the load position and its magnitude. Finding a good control command involves searching for the file name that corresponds to the load position and magnitude. Retrieving a good control command and sequence decreases the command search time to less than 1 min. Considering the search time distribution given in Fig. 14, this technique has the potential to avoid

search times of up to 1 h. Nevertheless, in situations where the only piece of information is the slope (unknown loads), the task is more difficult. A method for identifying loading would be necessary. Research into storing, retrieving and adapting good control commands and identifying load cases is underway. Using the control system to observe behavior due to small movement of active members may prove to be a good procedure for identifying loading.

Conclusions

Active control a tensegrity structure results in a lightweight reusable structural system that is capable of reacting to its environment. The challenges of creating an active tensegrity structure that satisfies serviceability criteria are threefold:

- Design and construction of an active control system for a complex structure;
- Behavior prediction of a geometrically nonlinear structure with strut and cable elements as well as active members; and
- Design of a control strategy for nonlinear, coupled and under-actuated systems that have no closed form solution for direct calculation of commands.

The results show that the control system strategy adopted in this tensegrity structure is capable of meeting a serviceability criterion. Combining a stochastic search via PGSL with dynamic relaxation enable identification of good control commands to maintain the slope of the upper layer under perturbations that involve asymmetric single and double vertical point loads. The quasistatic control strategy, consisting of splitting the full command into increments and applying them strut by strut with simultaneous measurements, leads to a safe procedure for meeting the serviceability criterion and provides opportunities by which to identify potentially better commands en route to the full command. Testing has demonstrated the robustness of the system. Iterative control, starting with a deformed shape and applying an additional command, has the potential to increase control effectiveness.

Storing good control commands and their associated control sequences speeds up the search by retrieving a previous command that is associated with the same loading. A multicriteria search may be useful to find commands that, for example, provide slope compensation while maintaining the most capacity to counteract additional future loads.

The work should contribute to developing a structure that, through integrating a control system, iterative control, and retrieving previous control commands, will improve its performance during service life.

Acknowledgments

The writers would like to thank the Swiss National Science Foundation for funding this research under contract and Maag Technic, Hi-Tech Engineering (Zurich), Lust-tec (Zurich), HBM (Darmstadt) and National Instruments for their support. They are also grateful to B. Domer, B. Raphael, Passera & Pedretti SA, S. Rossier, P. Gallay, M. Pascual and C. Gilliard for their contributions.

References

- Barnes, M. R. (1977). "Formfinding and analysis of tension space structures by dynamic relaxation." PhD thesis, The City University Press, London.
- Barnes, M. R. (1999). "Formfinding and analysis of tension space structures by dynamic relaxation." *Int. J. Space Struct.*, 14(2), 89–105.
- Bosch, R. (1993). Control area network (CAN) Specification 2.0 Part A.
- Djouadi, S. (1988). "Le contrôle des structures tensegrité et les systèmes tensegrité." Doctoral thesis, Laboratoire de Mécanique et Génie Civil Univ., Montpellier II, Montpellier, France, 134 (in French).
- Domer, B., Fest, E., Lalit, V., and Smith, I. F. C. (2003a). "Combining the dynamic relaxation method with artificial neural networks to enhance simulation of tensegrity structures." *J. Struct. Eng.*, 129(5), 672–681.
- Domer, B., Raphael, B., Shea, K., and Smith, I. F. C. (2003b). "A study of two stochastic search method for structural control." *J. Comput. Civ. Eng.*, 17(3), 132–141.
- Emmerich, G. D. (1964). "Construction de réseaux autotendants." *Brevet No. 1,377,290*, Brevet délivré par le Ministère de l'Industrie, Paris (in French).
- Fest, E. (2002). "Une structure active de type tensegrité." Doctoral thesis, Swiss Federal Inst. of Technology, Lausanne, Switzerland.
- Fest, E., and Smith, I. F. C. (2002). "Deux structures actives de type tensegrité." *Rev. Constr. Metal.*, 3(39), 19–27.
- Fest, E., Shea, K., Domer, B., and Smith, I. F. C. (2003). "Adjustable tensegrity structures." *J. Struct. Eng.*, 129(4), 515–526.
- Furuya, A. (1992). "Concept of deployable tensegrity structures in space applications." *Int. J. Space Struct.*, 7(2), 75–83.
- Ingber, E. D. (1998). "The architecture of life." *Sci. Am.*, 278(1), 30–39.
- Kanchanasaratool, N., and Williamson, D. (2002). "Modelling and control of class NSP tensegrity structures." *Int. J. Control*, 75(2), 123–139.
- Le Saux, C., Bouderbala, M., Cevaer, F., and Motro, R. (1999). "Strut-strut contact in numerical modeling of tensegrity system folding." *40th Anniversary of IASS, from recent past to next millenium*, International Association for Shell and Spatial Structures, Madrid, Spain, D1–D10.
- Micheletti, A. (2003). "The indeterminacy condition for tensegrity towers." *Rev. Fr. Génie Civ.*, 7(3), 329–342.
- Motro, R. (2002). "Tensegrity: The state of the art." *5th Int. Conf. on Space Structures*, G. A. R. Parke and P. Disney, eds., Telford, London, 97–106.
- Motro, R. (2003). "Tensegrité: Principe structural." *Rev. Fr. Génie Civ.*, 7(3), 251–266.
- Motro, R., and Raducanu, V. (2001). "Tensegrity systems and tensile structures." *Extended Abstracts, Int. Symp. on Theory, Design and Realization of Shell and Spatial Structures*, H. Kunieda, ed., Nagoya, Japan, 314–315.
- Murakami, H. (2001). "Static and dynamic analyses of tensegrity structures. Part 1. Nonlinear equations of motion." *Int. J. Solids Struct.*, 38(50), 3599–3613.
- Pedretti, M. (1998). (http://www.ppeng.ch/base_expo.htm).
- Pellegrino, S., and Calladine, C. R. (1986). "Matrix analysis of statically and kinematically indeterminate frameworks." *Int. J. Solids Struct.*, 22(4), 409–428.
- Radacanu, V., and Motro, R. (2001). "New tensegrity grids." *Int. Association for Shell and Spatial Structures Symp.*, H. Kuneida, ed., International Association for Shell and Spatial Structures, Madrid, Spain, 320–321.
- Raphael, B., and Smith, I. F. C. (2003). "A direct stochastic algorithm for global search." *J. Appl. Math. Comput.*, 146(2–3), 729–758.
- Robbin, J. L. (1996). *Engineering a new architecture*, Yale University Press, New Haven, Conn., 25–37.
- Rossier, S. (1993). "Optimization of cable structures using genetic algorithms." *Internal Rep.*, Swiss Federal Inst. of Technology, Lausanne, Switzerland.
- Saitoh, M., Okada, A., and Tabata, H. (2001). "Study on the structural characteristics of tensegric truss arch." *Int. Association for Shell and Spatial Structures Symp.*, H. Kunieda, ed., International Association for Shell and Spatial Structures, Madrid, Spain, 326–327.
- Shea, K., Fest, E., and Smith, I. F. C. (2002). "Developing intelligent tensegrity structures with stochastic search." *Adv. Eng. Inf.*, 16(1), 21–40.
- Skelton, R. E., Pinaud, J. P., and Mingori, D. L. (2001a). "Dynamics of the shell class of tensegrity structures." *J. Franklin Inst.*, 338, 255–338.
- Skelton, R. E., Helton, W.J., Adhikari, R., Pinaud, J. P., and Chan, W. (2001b). "An introduction to the mechanics of tensegrity structures." *Handbook on mechanical systems design*, 1–141.
- Sultan, C., Corless, M., and Skelton R. E. (2002). "Symmetrical reconfiguration of tensegrity structures." *Int. J. Solids Struct.*, 39, 2215–2234.
- Tibert, G. (2002). "Deployable tensegrity structures for space applications." PhD thesis, Dept. of Mechanics, Royal Inst. of Technology, Stockholm, Sweden.
- Vassart, N., Laporte, R., and Motro, R. (2000). "Determination of mechanism's order for kinematically and statically indetermined systems." *Int. J. Solids Struct.*, 37, 3807–3829.
- Wang, B.-B. (2002). "AP and ATP grids—Bridging tensegrity to cable strut." *5th Int. Conf. on Space Structures*, G. A. R. Parke, and P. Disney, eds. Telford, London, 5, 1200–1208.